Anthropocene Science (2023) 2:81–92
https://doi.org/10.1007/s44177-023-00051-7

ORIGINAL ARTICLE

Deforestation Drivers Across the Tropics and Their Impacts on Carbon Stocks and Ecosystem Services

Tobias Seydewitz[1,2] · **Prajal Pradhan**[1,3] · **David M. Landholm**[1,4] · **Juergen P. Kropp**[1,3,5]

Received: 1 August 2022 / Revised: 29 March 2023 / Accepted: 30 March 2023 / Published online: 17 April 2023

Abstract

Globally, deforestation produces anthropogenic greenhouse gas (GHG) emissions, contributing substantially to climate change. Forest cover changes also have large impacts on ecosystem services. Deforestation is the dominant type of land cover change in tropical regions, and this land cover change relates to distinct causes recognized as direct deforestation drivers. Understanding these drivers requires a significant effort. Further, GHG emissions due to deforestation are quantified only in terms of biomass removal, while linking emissions from soil organic carbon (SOC) loss to deforestation is lacking. A closer picture of associated ecosystem service changes due to deforestation is also needed. We analyze for 2001–2010: (1) the magnitudes of deforestation drivers, (2) the related carbon loss, and (3) the ecosystem service value change. On the global scale, agriculture (90.3%) is the primary deforestation driver, where grassland expansion contributed the most (37.5%). The deforestation drivers differ in magnitude and spatial distribution on the continental scale. The total carbon loss by biomass removal and SOC loss accounted for 8797 Mt C and 1185 Mt C, respectively. Furthermore, tropical deforestation caused the ESV loss of 408 billion Int.$ year^{-1}, while the resulting land cover has the ESV of 345 billion Int.$ year^{-1}. Our findings highlight that agriculture substantially contributes to global carbon loss and ecosystem service loss due to deforestation. The deforestation drivers differ in magnitude and distribution for different continents. Further, we highlight the danger of putting a monetary value on nature.

Keywords Deforestation · Soil carbon · Biomass · Land use change · Tropics · Emissions

1 Introduction

Tropical forests play a critical role in the global carbon cycle and are global biodiversity hotspots, presenting roughly 50% of terrestrial species and two-thirds of all plant species (Dirzo and Raven 2003). Globally, approximately 3.1% of the forest area has been lost between 1990 and 2015, of which around 35% of the deforestation occurred within the tropics (FAO 2016). Deforestation contributes to climate change, causes biodiversity loss, and degrades ecosystems significantly (Baccini et al. 2012; IPBES 2019). Between 2007 and 2016, forestry and other land use resulted in greenhouse gas (GHG) emissions of 5.8 ± 2.6 Gt CO_2eq year^{-1}, mostly due to deforestation (IPCC 2019; Rosenzweig et al. 2020). To achieve global climate targets, forestry, and other land use GHG emissions must decrease along a nonlinear trajectory and reach carbon neutrality by 2050 (Rockström et al. 2017). However, to successfully address this road map, improving our understanding of deforestation drivers is urgently needed.

The assessment of deforestation drivers is usually undertaken from two different approaches (Geist and Lambin 2002). Firstly, direct deforestation drivers refer to the land cover that replaces the forest cover after a deforestation event (e.g., pasture, cultivated land, urban area). Secondly, indirect drivers represent the root socio-economic causes underpinning these land cover changes. Globally,

✉ Prajal Pradhan
pradhan@pik-potsdam.de

1 Potsdam Institute for Climate Impact Research (PIK), Member of the Leibniz Association, P.O. Box 60 03, 14412 Potsdam, Germany

2 Eberswalde University for Sustainable Development (HNEE), Eberswalde, Germany

3 Bauhaus Earth gGmbH, Berlin, Germany

4 Climate Focus, Berlin, Germany

5 Institute for Environmental Science and Geography, University of Potsdam, Potsdam, Germany

the expansion of the agricultural frontier remains the single most important direct driver of deforestation (Curtis et al. 2018; Gibbs et al. 2010). Other direct drivers, such as timber and mining industries, also operate globally and play an essential role in deforestation (Asner et al. 2009; Edwards et al. 2014; Hosonuma et al. 2012). Progress in remote sensing and the availability of empirical data has fostered the research on direct deforestation drivers on a continental or regional scale (Austin et al. 2019; Curtis et al. 2018; De Sy et al. 2019; Hosonuma et al. 2012). Despite this progress, very few studies address deforestation causes systematically at a global level in a spatially explicit manner (Curtis et al. 2018). Most studies rely on methodologically inconsistent data coming from country reporting (FAO 2015). Furthermore, studies examining direct deforestation drivers in a spatially explicit manner are only available in a low resolution.

Total GHG emissions arising from deforestation can be broken down into three components: (i) emissions from biomass removal (Baccini et al. 2012), (ii) emissions resulting from loss of soil organic carbon (SOC) (Don et al. 2011), and (iii) emissions arising from the resulting land use (Avitabile et al. 2016). Studies that estimate the carbon loss by biomass removal on a global or regional scale are relatively common, with assessments ranging between 600 and 1400 Mt C year^{-1} for 2000–2010 period (Achard et al. 2014; Baccini et al. 2012; Houghton et al. 2012; Sy et al. 2015). However, the exploration of SOC loss resulting from land-use change through deforestation remains unknown at the global scale. Estimating these emissions is essential, given that tropical soils represent substantial carbon storage, accounting for 36–60% of the carbon stored in forests (Don et al. 2011).

Tropical ecosystems provide a crucial contribution to human well-being and the subsistence of current and future generations by providing regulatory, supporting, provisioning, and cultural services (Costanza et al. 1997). Deforestation and land cover changes lead to the widespread loss of ecosystem services by altering forest biomes. Therefore, it is crucial to evaluate these impacts in terms of GHG emissions and ecosystem service provisioning. Ecosystem service valuation is the attempt to assign a relative value to an ecosystem and its services. These values may be expressed in a wide range of different units, but monetary units are usually preferred due to easier communication (Costanza et al. 2014). The valuation of ecosystem services can raise public awareness of ecosystems as scarce resources, which should not be treated as free, inexhaustible goods (de Groot et al. 2012).

Song (2018) estimates an ESV loss of 550.7 billion Int.$ year^{-1} due to tropical deforestation. However, these ESVs do not consider ecosystem services from the resulting land use that replaces tropical forests. These studies miss the whole picture of ESV change and highlight the underlying danger of putting a monetary value on nature.

We aim to fill the research gaps presented above on the understanding of tropical deforestation drivers and associated GHG emissions and ESV change. For this, we investigate in a spatially explicit manner the following questions for the entire tropics between 23° North and 23° South: (1) What are the direct drivers of deforestation across different spatial scales? (2) What are the impacts of deforestation on carbon stocks resulting from biomass removal and SOC loss? (3) What are the magnitudes of the ESV change resulting from tropical deforestation?

2 Data and Methods

2.1 Tropical Deforestation and Drivers

We use the Global Forest Change (GFC) dataset (Hansen et al. 2013) and the global land cover GlobeLand30 (GL30) dataset (Chen et al. 2015) to scrutinize tropical deforestation and the related drivers (table S1). The GFC dataset provides annual global tree cover loss and gain data for the canopy density range from 0 to 100% between 2001 and 2012 and the tree cover for 2000 at a spatial resolution of 30 m. The GL30 dataset is a global land cover classification data for 2000 and 2010 at a spatial resolution of 30 m, consisting of ten distinct land cover types.

In the first step, we align and harmonize both datasets due to differences in their spatial properties. This step creates a set of similar meta-data raster images for each location in our study extent. We select the World Geodetic System 1984 (WGS84) as the target coordinate reference system and the bounding box of the GL30 tiles from 2010 as the target extent and resolution for the mosaic. The harmonization process determines for each selected template tile the intersecting tiles from each applied raster dataset. Next, the intersecting tiles are merged, re-projected, and clipped in terms of the mentioned template tile meta-data.

Second, we harmonize the tree cover definition between the GFC and the GL30 dataset. We combine the spatial information of GFC's tree cover loss and gain records and GL30's land cover classification to identify deforestation drivers. However, both differ in their definition of tree cover by varying canopy cover thresholds. GFC detects tree cover over the entire canopy density interval of (0%, 100%], while the GL30 threshold is set to >10% in sparse tree cover and >30% in terms of dense tree cover. To successfully extract stable land cover change by superimposing both datasets, we have to harmonize the tree cover definition among both datasets. We hypothesize that if both datasets have the same tree cover definition, they should agree if a non-forest state transition occurs. To harmonize the tree cover definition

between both datasets, we vary the GFC dataset's canopy density to determine which is most similar to the GL30's tree cover definition. We apply the Jaccard Index (JI) (Jaccard 1912) to measure tree cover similarity. It is a similarity measure between two pairs of a binary population. We use Eq. 1 to estimate the JI, where a is the magnitude of population agreement (i.e., presence of tree cover at the pixel level in both datasets), and b as well c are the magnitudes of population disagreement (i.e., either a tree cover record in GFC and not in GL30 or not in GFC but in GL30).

$$\mathrm{JI} = \frac{a}{a+b+c}. \tag{1}$$

We compute the JI for each GL30 and GFC tile pair for the canopy density set {0%, 10%, 20%, 30%}, where for each canopy density set, elements smaller than the threshold are excluded from the aggregation. After, we apply a two-sided and one-sided Wilcoxon signed-rank test (i.e., a non-parametric statistical hypothesis test) to determine which canopy density achieves the highest tree cover agreement between both datasets. We use the one-sided test to determine which canopy density achieves the highest agreement and the two-sided test to exclude equality between two pairs. Before statistical testing, we exclude all samples where the initial JI is zero since trees do not cover these tiles.

Third, to obtain the different deforestation driver types between 2001 and 2010, we select all forest loss from the GFC dataset within the target canopy density >10%. Next, the selected loss is superimposed by the land cover classification of the GL30 dataset from 2010. We obtain a dataset of classified forest loss by this process, which relates to the deforestation driver types in Table 1. To derive forest regrowth, we superimpose the obtained deforestation driver dataset by the GFC gain dataset. Some forest loss pixels (i.e., around 10%) are classified as forests by the GL30 dataset. Therefore, we reclassify all forest loss pixels assigned to this forest type. These pixels are clustered by applying the Hoshen–Kopelman algorithm, which aggregates single cells with similar properties to a larger cluster by applying a distance measurement to determine the neighbourhood (Hoshen 1998).

We use the Von Neumann neighbourhood rule for distance measurement, which selects a centre cell's four adjacent cells as its neighbours on a two-dimensional lattice. Next, the most frequent land cover type is determined within a 500 m side length square-sized buffer around the cluster centroid. Finally, the land cover type of the most frequent land cover type is assigned to the cluster. As described above, we introduce regrowth as a new land cover type from the GFC gain dataset. The land cover type regrowth accounts for tree crops like oil palm plantations or forestry activities. Further, this type could be the natural regeneration of tree cover after using the area for other purposes like shifting agriculture or just natural regrowth after non-anthropogenic forest disturbance (e.g., storm or fire). Forest loss classified as grassland accounts for expanding pastures (Graesser et al. 2015). Forest loss, classified as wetland and water, is due to inundation by lakes and rivers; therefore, it relates to natural changes (Sy et al. 2015).

To analyze the land cover change classification's reliability, we perform an accuracy assessment by applying random stratified sampling and estimate the user's, producer's, overall accuracy, and change area per deforestation driver with 95% confidence interval at global scale (Olofsson et al. 2014). For the sampling, we selected ten random raster tiles per continental region (Fig. S1). From each tile, we select 200 randomly classified tree cover losses. Next, we assigned a land cover change class to each sample by visually interpreting Google earth imagery. We used a pixel-based error matrix to derive the overall accuracy (rate of reference sites

Table 1 Direct deforestation driver classification scheme of this study

Type	Definition
Cultivated land	Used for agriculture, horticulture and gardens, including paddy fields, irrigated and dry farmland, vegetable and fruit gardens, etc
Regrowth	Canopy density >50%, inverse of forest loss
Grassland	Covered by natural grass with cover over 10%, etc
Shrubland	Covered by shrubs with cover over 30%, including deciduous and evergreen shrubs, and desert steppe with cover over 10%, etc
Wetland	Covered by wetland plants and water bodies, including inland marsh, lake marsh, river floodplain wetland, forest/shrub wetland, peat bogs, mangrove ansalt marsh, etc
Water bodies	In land area, including river, lake, reservoir, fish pond, etc
Artificial surfaces	Modified by anthropogenic influence, including all kinds of habitation, industrial and mining area, transportation facilities, and interiourban green zones and water bodies, etc
Bareland	With vegetation cover lower 10%, including desert, sandy fields, Gobi, bare rocks, saline and alkaline land, etc

Type is the land cover type that replaces the forest and the definition is the land cover type that fits into this class. The definitions relate to the land cover classification scheme of Chen et al. (2015)

correctly mapped) and producer's accuracy (per land cover type, the rate of correctly mapped samples).

For visualizing our results of deforestation and driver, we use a hexagonal grid and binning of the map data covered by the hexagon (Fig. S3). The cells cover an area of approximately 4.9 million ha at the equator. The hexagonal grid cells are scaled to represent the extent of deforestation, which is the ratio of total forest loss to tree cover 2000, and split into segments to show the driver of the binned area. We use our implementation in Python for the hexagonal gridding, binning, and splitting and QGIS for map composition.

2.2 Carbon Loss

For the evaluation of gross carbon loss through deforestation drivers, we use the following datasets: above-ground woody biomass density (AGB), global SOC map (GSOCmap), and intact forest landscape (IFL) (FAO & ITPS 2018; Harris et al. 2021; Potapov et al. 2017) (Table S1). The AGB dataset is a wall-to-wall map of above-ground woody biomass density at approximately 30 m resolution based on the methodology of Baccini et al. (2012). The GSOCmap provides data on the topsoil layer's soil organic carbon content between 0 and 30 cm at a spatial resolution of approximately 1 km. The IFL dataset records large patches of undisturbed primary forests and naturally treeless ecosystems that show no detectable human activity signs. All three datasets are spatially harmonized, similar to the above-described process, while we down-scaled the GSOCmap with the nearest neighbor resampling to match the other datasets' spatial resolution. Further, we use SOC change rates provided by Don et al. (2011) to evaluate the SOC loss by proximate deforestation drivers (Table S2). We assign the SOC change rates to deforestation driver types using the land cover change types.

We interpret the land cover change by a deforestation driver as the complete removal of the above-ground biomass to evaluate the carbon loss through biomass removal. We convert the AGB map's biomass density to carbon density by multiplying each pixel value by 0.5 as suggested by the dataset providers to calculate the carbon loss by deforestation drivers (Harris et al. 2021; Saatchi et al. 2011). Further, we calculate the area a pixel covers per raster tile to get the entire carbon content per grid cell by applying the Haversine equation, since in the WGS-84 projection the area is dependent on its geographical coordinate (Brinck et al. 2017). Next, we derive the below-ground biomass (BGB) by applying Eq. 2 from Mokany et al. (2006), which suggests that a power function better reflects relation between BGB and AGB than a linear regression. This power function is also used by many studies (Bernal et al. 2018; Pearson et al. 2017; Saatchi et al. 2011). We obtain the total carbon content of the biomass (BIO) by summing AGB and BGB.

$$\mathrm{BGB} = 0.489 \times \mathrm{AGB}^{0.89}. \quad (2)$$

To evaluate the carbon loss through SOC change by land cover change, we convert the per pixel carbon content of the GSOCmap to absolute carbon content by applying the Haversine equation to get the area a pixel covers per raster tile. After, we scrutinize the carbon losses for two different scenarios. For scenario one (SC1), we assume that all deforestation occurs in the primary forest. For the second scenario (SC2), we distinguish between a land cover change in a primary and secondary forest using the IFL dataset. We evaluated the SOC loss for two different scenarios because selecting primary forest based on the IFL dataset is a very conservative approach. This dataset only provides large patches (> 500 km^2) of forests and other natural ecosystems uninterrupted by anthropogenic activities (Potapov et al. 2017). Therefore, primary forest can still exist outside of these patches.

We use the natural earth dataset to estimate the soil organic and biomass carbon loss per continent and tropical country. We determine the gross carbon loss per deforestation driver for each country by accumulating the following deforestation driver types: cultivated land, regrowth, grassland, shrubland, artificial, and bare land. We select these types because they represent anthropogenic land cover change.

2.3 Ecosystem Service Values

We use the global ecosystem service unit values in 2007 Int$/year provided by Costanza et al. (2014) to scrutinize the ESV loss by direct deforestation drivers and the ESV of the resulting land cover (Table S3). We calculate the ESV loss by multiplying the forest loss area by deforestation driver types of cultivated land, regrowth, grassland, shrubland, artificial, and bareland with the tropical forest's ecosystem service unit value, which relates to the methodology of basic value transfer. Additionally, we evaluate the ESV gain by multiplying the representative ecosystem service unit value with the estimated area deforested by a deforestation driver. Our results are aggregated per continent and tropical country using the boundaries of the natural earth dataset.

3 Results

3.1 Tropical Deforestation and Drivers

On a global scale, the highest forest cover agreement between the GFC and GL30 datasets is within the canopy density interval of (10, 100] (Fig. S2). Our statistical test also shows that the tree cover agreement of this canopy density interval is significantly greater than the agreement of other

intervals (Table S4). Therefore, we use for the direct deforestation driver mapping all tree cover loss within the canopy density interval (10, 100].

Globally, approximately 77 million ha of tropical forest was lost between 2001 and 2010 (Fig. 1). The expansion of agricultural land causes approximately 90% of the deforestation. Table S5 lists the total forest loss and the main deforestation driver we obtained in our study disaggregated by country, continent, and global. Within agriculture, the expansion of grassland accounts for 37.5% of deforestation, followed by regrowth (29.96%) and cultivated land (22.82%). A minor deforestation driver is the expansion of artificial surfaces (0.48%). Other causes, like forest inundation, account for 1.56% of the tropical forest loss. However, the entire deforested area and distribution of drivers in terms of total share and spatial coverage vary per continental region (Fig. 2).

Approximately 39 million ha was deforested in South and North America between 2001 and 2010. The following four countries show large (i.e.,> 1 million ha) cumulative deforestation in these continents: Brazil (27.6 million ha), Paraguay (2.1 million ha), Bolivia (1.9 million ha), and Colombia (1. 6 million ha). For these continents, the primary deforestation driver is the expansion of grassland with a share of 46.64%, followed by cultivated land (24.04%) (Fig. 2). In Brazil, forest loss is primarily concentrated in the north of the country (Fig. 1). The forest loss in this region, also known as the arc of deforestation (Sy et al. 2015), can mainly be attributed to grassland expansion. In contrast, the expansion of cultivated land is mainly detected in the south of Brazil. In total, approximately 53% of the deforested land in Brazil is converted to grassland, while 20% can be attributed to cultivated land. The northern part of Paraguay, known as the Gran Chaco, shows extensive absolute deforestation, of which the expansion of cultivated land drives over a half. In Bolivia, tree cover loss is primarily concentrated at the country's centre, while the main deforestation driver is the expansion of cultivated land. On the country scale, the primary cause for tree cover loss (46.6%) in Bolivia is the expansion of cultivated land (Sy et al. 2015). In the north and south of Colombia, grassland expansion is the primary deforestation driver (Graesser et al. 2015). These regions represent large forest losses as well.

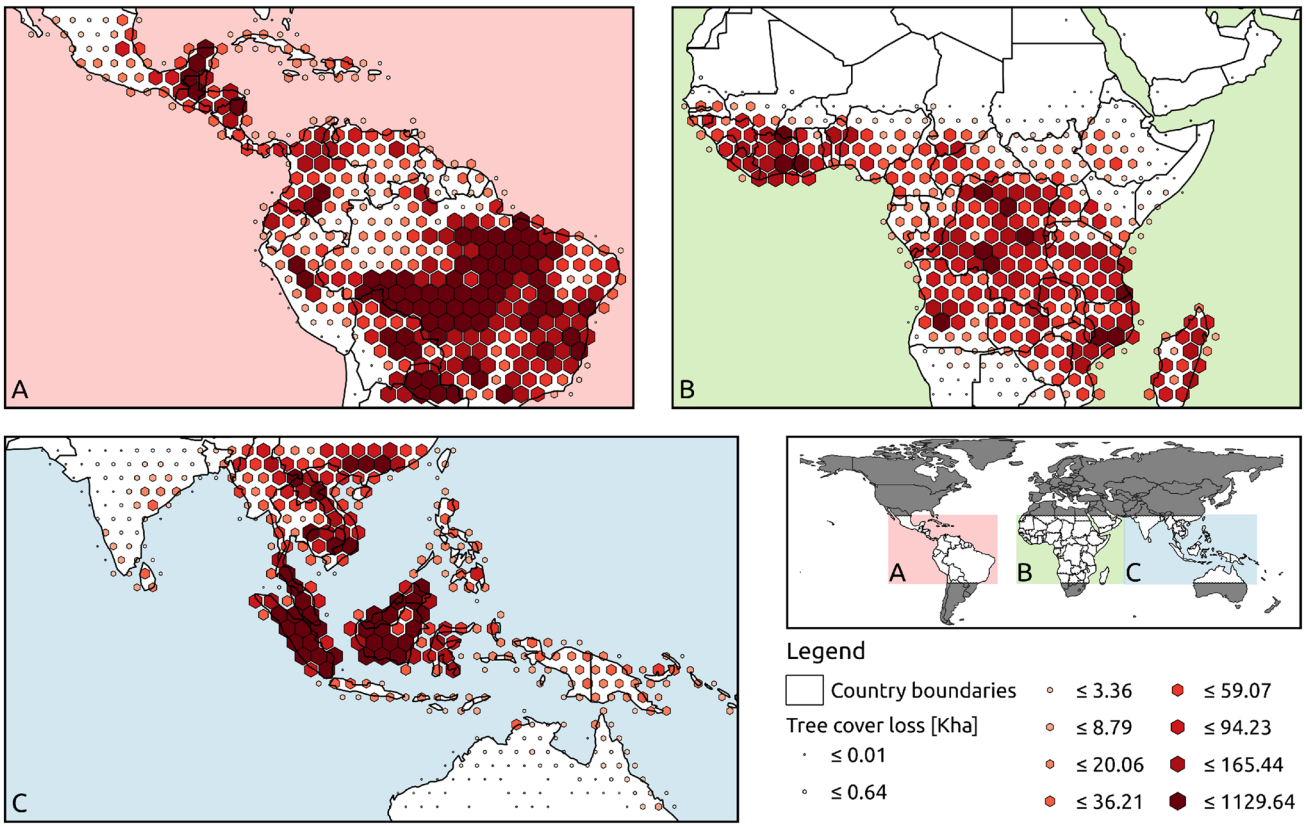

Fig. 1 The area of deforestation varies across the continents: **A** North and South America, **B** Africa, **C** and Asia/Oceania. Each hexagon shows by scaling and colour gradient the forest loss in Kha (10^3 ha) within the area covered by the grid cell. Each grid cell covers an area of approximately 4.9 million ha at the equator. Cells appearing not to cover the continents are a scaling artefact. Unscaled hexagons still intersect with the landmass (Fig. S3). Hexagonal gridding and binning are implemented in Python, and we use QGIS for map composition

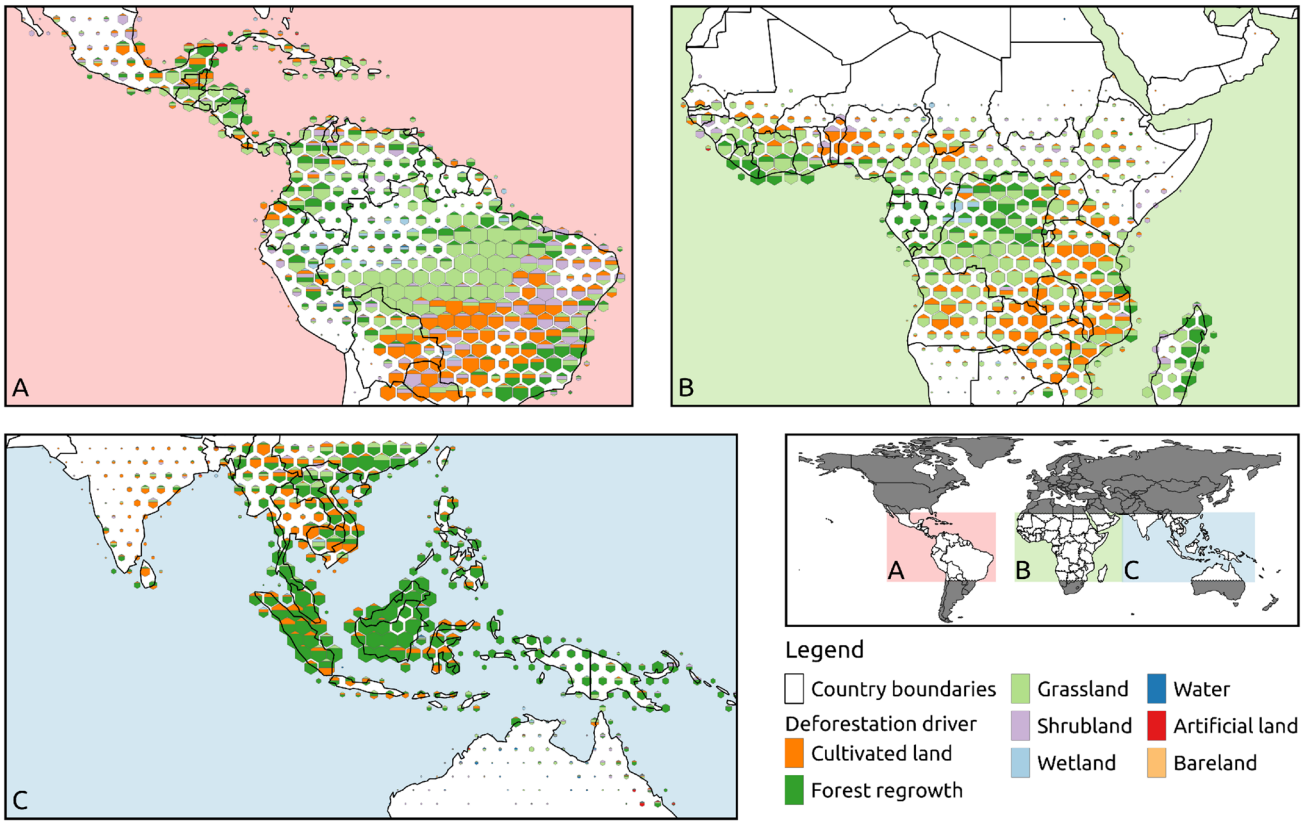

Fig. 2 The deforestation driver and their composition vary across the continents: **A** North and South America, **B** Africa, **C** and Asia/Oceania. Each hexagon's interior shows the composition of the most dominant deforestation driver sorted from bottom to top. Each grid cell covers an area of approximately 4.9 million ha at the equator. The hexagons' size corresponds to the forest loss within the region. Cells appearing not to cover the continents are a scaling artefact. Unscaled hexagons still intersect with the landmass (Fig. S3). Hexagonal gridding, binning and splitting are implemented in Python, and we use QGIS for map composition

We present our outcomes for Asia and Oceania together due to low country coverage in Oceania (Table S5). In both regions, a forest area of approximately 22 million ha was lost between 2001 and 2010. Our results suggest that 61.8% of the forest loss can be attributed to regrowth, while cultivated land and grassland (16% and 7.1%) expansion causes only a minority of the forest loss. The following four countries represent the top four in terms of total deforestation within the region: Indonesia (10.2 million ha), Malaysia (3.3 million ha), China (1.8 million ha), and Laos (0.8 million ha). More than half of the deforestation in Indonesia (76.13%), Malaysia (87.1%), and China (60.8%) can be attributed to regrowth dynamics (Table S5), which is also highlighted for Indonesia by Austin et al. (2019). Deforestation is mainly distributed over the islands of Sumatra and Borneo in Indonesia. Malaysian deforestation primarily centres on Borneo and continental Malaysia (Fig. 1). Roughly the same proportion of forest loss can be attributed to the expansion of cultivated land in China (18.01%), Indonesia (17.13%), and Laos (16.86%). In Laos, major deforestation is located in the north of the country.

In Africa, an area of 17 million ha was deforested within the period 2001–2010. The primary deforestation driver of this forest loss is the expansion of grassland (50%), followed by the expansion of cultivated land (25.01%). In Africa, the following four countries show the highest total deforestation: DR Congo (4.7 million ha), Mozambique (1.8 million ha), Tanzania (1.5 million ha), and Angola (1.4 million ha). In DR Congo and Angola, grassland expansion causes more than half of the deforestation (Fig. 2). Forest loss hotspots are scattered over the entire DR Congo, while the highest total forest loss can be observed in the country's south (Fig. 1). In Angola, deforestation has primarily occurred in the centre of the country. The expansion of cropland accounts for approximately one-third and two-fifths of the forest loss in Angola (34.23%), Mozambique (35.48%), and Tanzania (45.06%), respectively. In Mozambique, deforestation tends to be distributed in the country's north, while in Tanzania, substantial forest loss is primarily located in the south. In both countries, grassland expansion accounts for approximately two-fifths of the deforested areas.

Our mapping of direct deforestation drivers reaches an overall accuracy of approximately 87% (Tables S6 and S7). The following two land cover types have a producer's accuracy above 80%: cultivated land (90%), regrowth (84%) and grassland (90%). Shrubland achieves a producer's accuracy of approximately 80%, while permanent water bodies (67%) have a producer's accuracy. The lowest producer's accuracy is observed for the following three land cover types: wetland (54%), artificial (64%), and bareland (49%). Globally we estimate a changing area per deforestation driver in Kha of 17,451.9 (± 489.9), 25,296.8 (± 600.7), 27,412.2 (± 615.0), 5511.9 (± 357.4), 841.5 (± 166.7), 276.5 (± 98.4), 290.0 (± 96.1), and 60.7 (± 41.5) accounting for cropland, regrowth, grassland, shrubland, wetland, water, artificial, and bareland, respectively.

3.2 Carbon Loss

On a global scale, tropical deforestation accounts for a carbon loss of 8797.32 Mt C due to the removal of woody biomass between 2001 and 2010 (Table S7). The carbon loss induced by the SOC carbon change through land cover transitions is 1555.47 Mt C and 931.58 Mt C for scenario SC1 and SC2, respectively. Table S8 lists the carbon loss by related deforestation driver we obtained in our disaggregated by country, continent, and global. Dependent on the scenario, the total carbon loss caused by deforestation and land cover changes range between approximately 9734 Mt C and 10,352 Mt C. The primary source for biomass carbon loss is the expansion of grassland that accounts for approximately 40% of the carbon loss. In contrast, the transition of forests to cultivated land causes approximately 30–40% of the SOC loss. Comparable to the deforestation drivers, the carbon loss patterns varying across the study region, dependent on the selected scale.

North and South America show the greatest carbon loss among the continents (Fig. 3). The removal of above-and below-ground biomass accounts for approximately 4385 Mt C. For scenario SC1 and SC2, SOC loss range between 836.51 and 568.48 Mt C, respectively (Table S7). Transitions of forest cover to grassland, causing over a half (2473.9 Mt C) of the continental carbon loss by removing the woody above-and below-ground biomass. The expansion of grassland is also the primary driver of SOC loss, which accounts for 393.76 Mt C and 269.14 Mt C for scenarios one and two. The following countries represent the top four biomass carbon loss: Brazil (3231.8 Mt C), Bolivia (219.1 Mt C), Colombia (196.69 Mt C), and Peru (140.41 Mt C). In Brazil and Colombia, the leading cause for biomass carbon loss is the transition of forest cover to grassland, while in Bolivia, the primary source is the expansion of cultivated land. The carbon loss in Peru can mainly be attributed to the establishment of regrowth. The most immense SOC loss for scenario

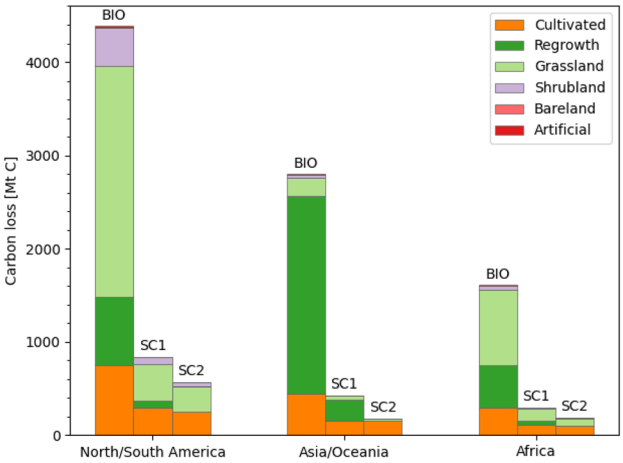

Fig. 3 Carbon loss through removal of above- and below-ground biomass (BIO) and soil organic carbon change (under scenario SC1 and SC2) on the continental scale per dis-aggregated deforestation driver. In scenario SC1, all land cover changes occurred in the primary forest. We distinguished between land cover change in primary and secondary forest in scenario SC2. Carbon loss by bareland is not visible in the figure because it is <1 Mt C but depicted in table S7

SC1 and SC2 is observed in the following four American countries: Brazil (580.96 Mt C, 408.46 Mt C), Bolivia (59.1 Mt C, 42.24 Mt C), Paraguay (38.86 Mt C, 30.67 Mt C), and Colombia (34.86 Mt C, 15.2 Mt C). Grassland is the primary cause of SOC loss in Brazil and Colombia, while the expansion of cultivated land is the primary source of SOC loss in Paraguay and Bolivia.

In Asia and Oceania, the gross carbon loss from biomass removal and SOC ranges between 2915.22 Mt C and 3163.44 Mt C. The majority of biomass removal is caused by the expansion of regrowth, accounting for 2056.91 Mt C of carbon loss. The second largest source for carbon loss is the expansion of cultivated land followed by grassland. For SOC loss, cultivated land and grassland are the primary sources as well. The following four countries contribute most to the continental gross carbon loss through biomass removal: Indonesia (1421.09 Mt C), Malaysia (493.09 Mt C), China (241.99 Mt C), and Laos (120.97 Mt C). In all four countries, regrowth expansion is the primary source of above- and below-ground biomass carbon loss. SOC loss in scenario SC1 is primarily distributed over the following countries: Indonesia (170.46 Mt C), Malaysia (75.71 Mt C), China (45.28 Mt C), and Vietnam (25.28 Mt C). Regrowth dynamics are the primary cause of these carbon losses in Indonesia, Malaysia, and China, while the forest transition to cultivated land is the primary source in Vietnam. The following four countries are the primary sources for carbon loss if these are calculated in line with scenario SC2: Indonesia (80.67 Mt C), China (17.64 Mt C), Vietnam (15.27 Mt C), and Cambodia (16.74 Mt C). A primary cause for this SOC

carbon loss is the expansion of cultivated land in all four countries.

For Africa, the gross carbon loss by biomass removal accounts for 1607.54 Mt C, while SOC loss is 292.58 Mt C and 184.94 Mt C for scenario SC1 and SC2, respectively. At the continental scale, the primary source of biomass removal is the expansion of grassland. The same account for SOC loss under scenario SC1, while SOC loss calculated in line with scenario SC2 is primarily driven by the forest's transition to cultivated land. Substantial carbon loss through biomass removal can be observed primarily in DR Congo (623.3 Mt C), Mozambique (138.64 Mt C), Madagascar (128.48 Mt C), Tanzania (91.51 Mt C). The carbon loss of the first two countries plus Tanzania is dominated by the expansion of grassland, while in Madagascar, the primary cause for biomass carbon losses is regrowth dynamics. Substantial SOC loss can be observed in the following four countries: DR Congo (81.29 Mt C, 55.66 Mt C), Mozambique (34.58 Mt C, 22.79 Mt C), Zambia (16.78 Mt C, 21.74 Mt C), and Tanzania (21.72 Mt C, 16.11 Mt C). In the last three countries, the carbon loss is primarily dominated by the expansion of cultivated land, while grassland transitions are the primary cause of SOC loss in DR Congo.

3.3 Ecosystem Service Values

Between 2001 and 2010, tropical deforestation accounts for an ESV loss of approximately 408 billion Int.$/year, while the ESV gain through land cover change is approximately 345 billion Int.$/year. Table S9 lists ESV loss and gain related to the deforestation driver we obtained in our study disaggregated by country, continent, and global. The transition of forests to grassland contributes the most to the ESV losses with about 155 billion Int.$/year, while the largest net gain can be observed for transitions to cultivated land that account for approximately 3 billion Int.$/year.

On a continental scale, the most substantial ESV loss is present in North and South America, accounting for the loss of 207 billion Int.$/year (Fig. 4). For the following four countries, we observed the highest ESV loss over the Americas: Brazil, Paraguay, Bolivia, and Colombia. In Brazil, the ESV loss through deforestation is about 146 billion Int.$/year, while the largest ESV gain can be attributed to the conversion of forest areas to grassland (60 billion Int.$/year). For Bolivia and Colombia, the losses are approximately 10 and 8 billion Int.$/year, while in Bolivia, the ESV gain is mainly attributed to cultivated land conversions (5 billion Int.$/year) and in Colombia fostered by grassland and regrowth transitions (2 billion Int.$/year). The loss of ESV is about 11 billion Int.$/year in Paraguay, while conversions to cultivated land are the most relevant gains (7 billion Int.$/year).

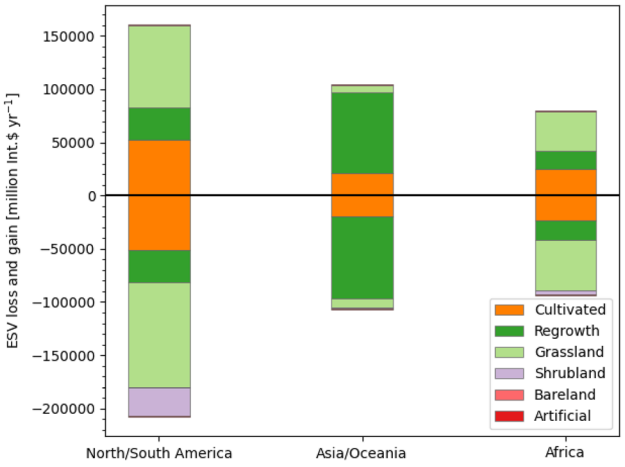

Fig. 4 Ecosystem service value (ESV) loss and gain on a continental scale in Int.$ year^{-1} per dis-aggregated direct deforestation drivers. Bars with negative values show ESV loss, while bars with positive values represent the gain

In Asia and Oceania, the ESV loss and gain account for 107 billion and 104 billion Int.$/year. Over the study period, the most substantial ESV loss is in Indonesia, with about 54 billion Int.$/yr. The expansion of regrowth primarily drives this loss. Similar ESV dynamics can also be observed in Malaysia, China, and Laos.

For Africa, we estimate the ESV loss of 93 billion Int.$/year and the ESV gain of 80 billion Int.$/year through land cover changes. The largest ESV loss can be attributed to the conversion of forest cover to grassland, which accounts for 48 billion Int.$/year, respectively. In Africa, transitions of forests to cultivated land translate to a more gain in the ESV than the loss in the monetary term. However, forest ecosystem services could not be replaced and compensated by the ecosystem services from cultivated land. The following four African countries contribute most to the continental ESV loss: DR Congo (24 billion Int.$/year), Mozambique (9 billion Int.$/year), Tanzania (7 billion Int.$/year), and Angola (7 billion Int.$/year). Most of this loss is driven by the expansion of grassland and cultivated land, while these transitions also represent major ESV gains.

4 Discussion

This study scrutinises the distribution of direct deforestation drivers across the tropics. Further, we evaluate carbon loss and changes in ESV due to tropical deforestation. Our study brings several new insights into understanding the drivers and impacts of tropical deforestation between 2001 and 2010. These insights are crucial for deriving forest-based measures for limiting global warming well below 2°C and

overall sustainable transformation, e.g., to achieve Sustainable Development Goals (SDGs).

First, our study highlights the variation in deforestation drivers across regions. For example, deforestation resulted in expanding cultivated land (24%) and pasture (46%) in North and South America. In contrast, regrowth occurred after most deforestation in Asia. This regrowth could relate to the large amounts of newly established tree crops in this region (Austin et al. 2019; De Sy et al. 2019). These findings address our first research question on deforestation drivers across spatial scales. Agriculture is the most relevant deforestation driver globally, accounting for approximately 90% of the forest loss. This deforestation can also be linked to the growing food trade (Foong et al. 2022). Therefore, sustainable transformation of food systems is essential to reduce deforestation and explore synergies between achieving zero hunger (SDG2) and conservation of life on land (SDG15). Currently, protecting biodiversity and natural habitats (SDG Target 15.5) is one of the challenging aims of the 2030 Agenda for Sustainable Development (Anderson et al. 2022). Moreover, our global estimate on forest loss due to agriculture is larger than the estimates from previous studies, i.e., 85% (Hosonuma et al. 2012) and 77% (Curtis et al. 2018) of the deforested area. These differences may come from our higher-resolution analysis to detect deforestation or the usage of different datasets and also the use of different definitions of agriculture, as mentioned previously.

Second, we present fine-grained insights into deforestation drivers' continental and regional distribution. For example, our study highlights that although Brazil presents the most severe deforestation countrywide, forests' conversion into pastures dominates its northern part. This conversion pattern is also reported by other studies (Graesser et al. 2015; Sy et al. 2015). Similarly, our study shows large expansions of cultivated land into forests in the centre of Bolivia. These understandings of a variation in deforestation drivers within a country help tailor policies, targeting specific drivers to halt deforestation. For example, our findings provide location-specific deforestation drivers that must be tackled to meet the Bonn Challenge's goal to restore degraded and deforested areas and the Kunming-Montreal Global Biodiversity Framework target to protect 30% of Earth's lands. Moreover, our research emphasises the need for targeted frameworks [Reducing Emissions from Deforestation and forest Degradation (REDD+), Latin American and Caribbean Initiative 20 × 20] to protect forests from expansion and conversion to agriculture. To successfully implement these frameworks, they must address location-specific deforestation drivers that may vary within a country. Their success is critical in the background of climate change mitigation and the call of the IPCC for reduced deforestation and afforestation to limit global warming to 1.5 °C or well below 2 °C (IPCC 2014).

Third, our study captures a more holistic picture of carbon loss by including soil organic carbon losses associated with deforestation, answering our second research question. Our estimates of carbon loss account for removing forest biomass and SOC loss due to land-use change; we also link the carbon loss to the deforestation drivers. Between 2001 and 2010, we estimate the total carbon loss of 8797 Mt C due to biomass removal by anthropogenic deforestation activities. This value is slightly lower than the estimates of existing literature that range between 10,000 and 11,400 Mt C (Baccini et al. 2012; Houghton et al. 2012). This difference may be explained due to the overestimation of carbon loss by the previous studies based on coarse resolution data and differing estimates of total forest loss. Additional to biomass removal, land-use change resulting from deforestation also contributed to 1185–1833 Mt C of the SOC loss during the study period. So far, this emission from SOC changes due to deforestation is not included in the carbon accounting, underestimating the total carbon loss due to deforestation by 13–20%.

Fourth, our study also provides a holistic picture of ESV changes due to deforestation, answering our third research question. We account for the loss of ESV due to deforestation and ESV of the resulting land use. Our study estimates deforestation accounts for the ESV loss of 408 billion Int.$/year. This value is close to the estimate of a loss of 550 billion Int.$/year by Song (2018). Additionally, we estimate the ESV gain of 345 billion Int.$/year by land use that replaces forest. That means ESV loss through deforestation could be close to the ESV gain from the resulting land use. These findings reveal the need to take the ecosystem service valuation approach cautiously because deforestation consists of two components—the ESV loss through deforestation and gain by new land cover types. The subsequent land use cannot replace ecosystem services and biodiversity loss due to deforestation. However, the monetary evaluation of ecosystem services might depict similar values, giving a wrong impression. Therefore, our study highlights the underlying danger of putting the monetary value on nature, giving the impression that ecosystem services are replaceable.

Our study also has a few limitations. First, we do not capture the dynamic dimension of deforestation drivers, e.g., the shift of forest to pasture, followed by a conversion to other land use. Nevertheless, our deforestation drivers' results are still valid because our study focuses on capturing the initial reason for deforestation. Second, we cannot distinguish between regrowth by establishing tree crops, forestry activities, or natural regeneration. For example, Chen et al. (2019) highlighted that greening in China is related to its ambitious afforestation programs. Nevertheless, most regrowth is related to tree crops, mainly oil palm plantations, in many countries. Third, our study estimates only the gross carbon loss through deforestation but not the carbon gain by the subsequent land use.

Additionally, our insights for carbon losses by SOC change should be understood as a rough estimate due to the low coverage of land cover change coefficients (Don et al. 2011). Similarly, we assume the removal of above- and below-ground biomass following the approach of Pearson et al. (2017). However, some below-ground biomass may remain in the deforested areas depending on substituting land use. Fourth, our estimates on ESV changes could be more precise by taking country-specific values instead of global ones. However, country-specific values are not available in sufficient coverage Costanza et al. (2014). Moreover, we estimate ESV changes to highlight the potential pitfall of putting a monetary value on nature. Fifth, the study results are only up to 2010 due to the unavailability of recent data at the time of the study. However, the study can still serve as an example of updating data to a more recent period, given that recent data has become available. Despite the limitations, the study provides valuable insights into different deforestation dynamics such as drivers, carbon loss, and ecosystem degradation, which are general impacts of deforestation even for the last decade, 2011–2020. Finally, our study points to agriculture as the primary deforestation driver, which is still the leading cause of deforestation (Curtis et al. 2018).

To limit global warming well below 2 °C as envisioned by the Paris Agreement, emissions from deforestation need to reduce to zero. Simultaneously, carbon sequestration from afforestation and sustainable land management needs to increase (Rockström et al. 2017). REED+ is mentioned as an instrument to address these needs in Nationally Determined Contributions of many countries (Hein et al. 2018). For a good implementation of instruments like REDD+, our study explains deforestation drivers at a high spatial resolution. Our study also fosters implementing the UN goals for sustainably managed forests until 2030 (UN 2019). By scrutinising the global deforestation driver dynamics, we directly contribute to the vital goal of providing relevant, accessible forest-related information. Further, we highlight that agriculture and its expansion into forested areas must be stopped actively to prevent ongoing deforestation. Therefore, it is required to include agriculture in decision-making, land-use planning, and other demand-side management strategies to ensure food security, such as avoiding food waste and changing diets (Bodirsky et al. 2019; Landholm et al. 2019b). Further, conflict prevention and avoidance help to exclude these as an additional crucial underlying driver of deforestation (Landholm et al. 2019a). Moreover, overall sustainable development should explore strategies that will synergise the conservation of life on land (SDG15) and other SDGs, opposite to the current situation (Warchold et al. 2022).

5 Conclusion

Our study highlights the variation of deforestation drivers across regions and countries and their considerable impact on carbon loss and ecosystem degradation. Each country must target its policy toward individual deforestation drivers for conserving forests. Halting tropical deforestation is crucial for climate change mitigation and conserving biodiversity and ecosystem services, and it could also contribute to rescuing the 2030 Agenda from failing (Pradhan 2023). However, implementing conservation interventions requires further understanding of deforestation mechanisms, including its indirect drivers, i.e., socio-economic causes, and exploring win-win solutions with other development goals. Future research can apply a multi-method approach to understand the root causes of deforestation, and this approach can consist of periodically updated datasets on direct deforestation drivers and stakeholder interactions.

Supplementary Information The online version contains supplementary material available at https://doi.org/10.1007/s44177-023-00051-7.

Funding Information Open Access funding enabled and organized by Projekt DEAL. This work was supported by Bundesministerium für Umwelt, Naturschutz, Bau und Reaktorsicherheit with funding for the Sustainable Amazonian Landscapes project (Grant number: 42206-6157) and by Bundesministerium für Bildung, Wissenschaft, Forschung und Technologie with funding for the BIOCLIMAPATHS project (Grant agreement No. 01LS1906A) under the Axis-ERANET call.

Data Availability The data produced by this study have been included as electronic Supporting Information.

Declarations

Conflict of interest The authors declare that they have no conflict of interest.

References

Achard F, Beuchle R, Mayaux P, Stibig H-J, Bodart C, Brink A, Simonetti D (2014) Determination of tropical deforestation rates and related carbon losses from 1990 to 2010. Glob Change Biol 20(8):2540–2554. https://doi.org/10.1111/gcb.12605

Anderson CC, Denich M, Warchold A, Kropp JP, Pradhan P (2022) A systems model of sdg target influence on the 2030 agenda for sustainable development. Sustain Sci 17(4):1459–1472. https://doi.org/10.1007/s11625-021-01040-8

Asner G, Rudel T, Aide T, Defries R, Emerson R (2009) A contemporary assessment of change in humid tropical forests. Conserv Biol 23(6):1386–1395. https://doi.org/10.1111/j.1523-1739.2009.01333.x

Austin KG, Schwantes A, Gu Y, Kasibhatla PS (2019) What causes deforestation in Indonesia? Environ Res Lett 14(2):024007. https://doi.org/10.1088/1748-9326/aaf6db

Avitabile V, Schultz M, Herold N, de Bruin S, Pratihast AK, Manh CP, Herold M (2016) Carbon emissions from land cover change in Central Vietnam. Carbon Manag 7(5–6):333–346. https://doi.org/10.1080/17583004.2016.1254009

Baccini A, Goetz SJ, Walker WS, Laporte NT, Sun M, Sulla-Menashe D, Houghton RA (2012) Estimated carbon dioxide emissions from tropical deforestation improved by carbon-density maps. Nat Clim Change 2(3):182–185. https://doi.org/10.1038/nclimate1354

Bernal B, Murray LT, Pearson TR (2018) Global carbon dioxide removal rates from forest landscape restoration activities. Carbon Balance Manag 13(1):1–13. https://doi.org/10.1186/s13021-018-0110-8

Bodirsky BL, Pradhan P, Springmann M (2019) Reducing ruminant numbers and consumption of animal source foods are aligned with environmental and public health demands. J Sustain Organic Agric Syst 69(1):25–30. https://doi.org/10.3220/LBF1581688226000

Brinck K, Fischer R, Groeneveld J, Lehmann S, Dantas De Paula M, Pütz S, Huth A (2017) High resolution analysis of tropical forest fragmentation and its impact on the global carbon cycle. Nat Commun 8:14855. https://doi.org/10.1038/ncomms14855

Chen J, Chen J, Liao A, Cao X, Chen L, Chen X, Mills J (2015) Global land cover mapping at 30m resolution: a POK-based operational approach. ISPRS J Photogramm Remote Sens 103:7–27. https://doi.org/10.1016/j.isprsjprs.2014.09.002

Chen C, Park T, Wang X, Piao S, Xu B, Chaturvedi RK et al (2019) China and India lead in greening of the world through land-use management. Nat Sustain 2(2):122–129. https://doi.org/10.1038/s41893-019-0220-7

Costanza R, D'Arge R, de Groot R, Farber S, Grasso M, Hannon B, van den Belt M (1997) The value of the world's ecosystem services and natural capital. Nature 387:253–260

Costanza R, de Groot R, Sutton P, van der Ploeg S, Anderson SJ, Kubiszewski I, Turner RK (2014) Changes in the global value of ecosystem services. Glob Environ Change 26(1):152–158. https://doi.org/10.1016/j.gloenvcha.2014.04.002

Curtis PG, Slay CM, Harris NL, Tyukavina A, Hansen MC (2018) Classifying drivers of global forest loss. Science 361(6407):1108–1111. https://doi.org/10.1126/science.aau3445

De Sy V, Herold M, Achard F, Avitabile V, Baccini A, Carter S, Verchot L (2019) Tropical deforestation drivers and associated carbon emission factors derived from remote sensing data. Environ Res Lett 14(9):094022. https://doi.org/10.1088/1748-9326/ab3dc6

de Groot R, Brander L, van der Ploeg S, Costanza R, Bernard F, Braat L, van Beukering P (2012) Global estimates of the value of ecosystems and their services in monetary units. Ecosyst Serv 1(1):50–61. https://doi.org/10.1016/j.ecoser.2012.07.005

Dirzo R, Raven PH (2003) Global state of biodiversity and loss. Annu Rev Environ Resour 28(1):137–167. https://doi.org/10.1146/annurev.energy.28.050302.105532

Don A, Schumacher J, Freibauer A (2011) Impact of tropical land-use change on soil organic carbon stocks—a meta-analysis. Glob Change Biol 17(4):1658–1670. https://doi.org/10.1111/j.1365-2486.2010.02336.x

Edwards DP, Sloan S, Weng L, Dirks P, Sayer J, Laurance WF (2014) Mining and the African environment. Conserv Lett 7(3):302–311. https://doi.org/10.1111/conl.12076

FAO (2015) Global Forest Resources Assessment 2015 (Tech. Rep.). FAO, Rome

FAO (2016) Global forest resources assessment 2015 (Tech. Rep.). Food and Agriculture Organization of the United Nations

FAO & ITPS (2018) Global Soil Organic Carbon Map V1.0. Food and Agriculture Organization of the United Nations. http://54.229.242.119/GSOCmap/. Accessed 4 Dec 2018

Foong A, Pradhan P, Frör O, Kropp JP (2022) Adjusting agricultural emissions for trade matters for climate change mitigation. Nat Commun 13(1):3024. https://doi.org/10.1093/nsr/nwad015

Geist HJ, Lambin EF (2002) Proximate causes and underlying driving forces of tropical deforestation. Bioscience 52(2):143. https://doi.org/10.1641/0006-3568(2002)052[0143:PCAUDF]2.0.CO;2

Gibbs HK, Ruesch AS, Achard F, Clayton MK, Holmgren P, Ramankutty N, Foley JA (2010) Tropical forests were the primary sources of new agricultural land in the 1980s and 1990s. Proc Natl Acad Sci 107(38):16732–16737. https://doi.org/10.1073/pnas.0910275107

Graesser J, Aide TM, Grau HR, Ramankutty N (2015) Cropland/pastureland dynamics and the slowdown of deforestation in Latin America. Environ Res Lett 10(3):034017. https://doi.org/10.1088/1748-9326/10/3/034017

Hansen MC, Potapov PV, Moore R, Hancher M, Turubanova SA, Tyukavina A, Townshend JRG (2013) High-resolution global maps of 21st-century forest cover change. Science 342(6160):850–853. https://doi.org/10.1126/science.1244693

Harris NL, Gibbs DA, Baccini A, Birdsey RA, de Bruin S, Farina M, Tyukavina A (2021) Global maps of twenty-first century forest carbon fluxes. Nat Clim Change 11(3). https://doi.org/10.1038/s41558-020-00976-6. https://climate.globalforestwatch.org Accessed 4 Dec 2018

Hein J, Guarin A, Frommé E, Pauw P (2018) Deforestation and the Paris climate agreement: An assessment of redd+ in the national climate action plans. Forest Policy Econ 90:7–11. https://doi.org/10.1016/j.forpol.2018.01.005

Hoshen J (1998) On the application of the enhanced Hoshen-Kopelman algorithm for image analysis. Pattern Recogn Lett 19(7):575–584. https://doi.org/10.1016/S0167-8655(98)00018-X

Hosonuma N, Herold M, De Sy V, De Fries RS, Brockhaus M, Verchot L, Romijn E (2012) An assessment of deforestation and forest degradation drivers in developing countries. Environ Res Lett 7(4):044009. https://doi.org/10.1088/1748-9326/7/4/044009

Houghton RA, House JI, Pongratz J, van der Werf GR, DeFries RS, Hansen MC, Ramankutty N (2012) Carbon emissions from land use and land-cover change. Biogeosciences 9(12):5125–5142. https://doi.org/10.5194/bg-9-5125-2012

IPBES (2019) Summary for policymakers of the global assessment report on biodiversity and ecosystem services of the Intergovernmental Science-Policy Platform on Biodiversity and Ecosystem Services (Tech. Rep.). IPBES

IPCC (2014) Climate change 2014: Synthesis Report. Contribution of Working Groups I, II and III to the Fifth Assessment Report of the Intergovernmental Panel on Climate Change [Core Writing Team, R.K. Pachauri and L.A. Meyer (eds.)] (Tech. Rep.). GenevaIPCC. https://doi.org/10.1017/CBO9781107415324

IPCC (2019) Climate Change and Land: An IPCC Special Report on climate change, desertification, land degradation, sustainable land management, food security, and greenhouse gas fluxes in terrestrial ecosystems. Chapter 2: Land-Climate Interactions. [Coordinating Lead Authors: G. Jia and E. Shevliakova; Lead Authors: P. Artaxo, N. De Noblet-Ducoudré, R. Houghton, K. Kitajima,

C. Lennard, A. Popp, A. Sirin, R. Sukumar, L. Verchot](Tech. Rep.). GenevaIPCC

Jaccard P (1912) The distribution of the flora in the Alpine zone. New Phytol 11(2):37–50

Landholm DM, Pradhan P, Kropp JP (2019a) Diverging forest land use dynamics induced by armed conflict across the tropics. Glob Environ Change 56:86–94. https://doi.org/10.1016/j.gloenvcha.2019.03.006

Landholm DM, Pradhan P, Wegmann P, Sánchez MA, Salazar JCS, Kropp JP (2019b) Reducing deforestation and improving livestock productivity: Greenhouse gas mitigation potential of silvopastoral systems in Caquetá. Environ Res Lett. https://doi.org/10.1088/1748-9326/ab3db6

Mokany K, Raison RJ, Prokushkin AS (2006) Critical analysis of root-shoot ratios in terrestrial biomes. Glob Change Biol 12(1):84–96. https://doi.org/10.1111/j.1365-2486.2005.001043.x

Olofsson P, Foody GM, Herold M, Stehman SV, Woodcock CE, Wulder MA (2014) Good practices for estimating area and assessing accuracy of land change. Remote Sens Environ 148:42–57. https://doi.org/10.1016/j.rse.2014.02.015

Pearson TR, Brown S, Murray L, Sidman G (2017) Greenhouse gas emissions from tropical forest degradation: an underestimated source. Carbon Balance Manag 12(1):1–11. https://doi.org/10.1186/s13021-017-0072-2

Potapov P, Hansen MC, Laestadius L, Turubanova S, Yaroshenko A, Thies C, Esipova E (2017) The last frontiers of wilderness: Tracking loss of intact forest landscapes from 2000 to 2013. Sci Adv. https://doi.org/10.1126/sciadv.1600821

Pradhan P (2023) A threefold approach to rescue the 2030 agenda from failing. Natl Sci Rev. https://doi.org/10.1093/nsr/nwad015

Rockström J, Gaffney O, Rogelj J, Meinshausen M, Nakicenovic N, Schellnhuber H (2017) A roadmap for rapid decarbonization. Science 355(6331):1269–1271. https://doi.org/10.1126/science.aah3443

Rosenzweig C, Mbow C, Barioni LG, Benton TG, Herrero M, Krishnapillai M, Portugal-pereira J (2020) Climate change responses benefit from a global food system approach. Nat Food 1:1–4. https://doi.org/10.1038/s43016-020-0031-z

Saatchi SS, Harris NL, Brown S, Lefsky M, Mitchard ETA, Salas W, Morel A (2011) Benchmark map of forest carbon stocks in tropical regions across three continents. Proc Natl Acad Sci 108(24):9899–9904. https://doi.org/10.1073/pnas.1019576108

Song X-P (2018) Global estimates of ecosystem service value and change: taking into account uncertainties in satellite-based land cover data. Ecol Econ 143:227–235. https://doi.org/10.1016/j.ecolecon.2017.07.019

Sy VD, Herold M, Achard F, Beuchle R, Clevers JGPW, Lindquist E, Verchot L (2015) Land use patterns and related carbon losses following deforestation in South America. Environ Res Lett 10(12):124004. https://doi.org/10.1088/1748-9326/10/12/124004

UN (2019) Global forest goals and targets of the un strategic plan for forests 2030 (resreport). United Nations

Warchold A, Pradhan P, Thapa P, Putra MPIF, Kropp JP (2022) Building a unified sustainable development goal database: why does sustainable development goal data selection matter? Sustain Dev 30(5):1278–1293. https://doi.org/10.1002/sd.2316